Sensitivity Enhancement of Point-of-Care for Cardiac Markers Detection using Micro-Impedimetric Immunosensor Arrays

Eyad M. Hamad *Member IEEE*, Samer I. Al-Gharabli, and James A. McLaughlin

***Abstract*—This paper describes the development and characterisation of a novel, electrical impedance spectroscopy-based (EIS) immunosensor array for point-of-care applications. EIS is a highly sensitive, label-free, real time technique suitable for single use, point-of-care cardiac marker detection devices. However, the underlying source of the observed change in EIS immunoassay response has not been well characterised or understood. A full understanding of the relationship between target binding and impedance response would significantly advance biosensor design and most probably increase detection limit sensitivity. The development of micro-/nano- structured electrodes for multi-frequency EIS procedure propose substantial benefits over classical macro-structured systems.**

Countless manipulations of electrode features and inter-electrode spacing will enhance the electrode surface area, increase the charge-transfer resistance and reduce the double-layer capacitance. These in turn give rise to improved signal-to-noise ratios, therefore affording greater sensitivity, lower detection limits and faster detection times.

The sensor sensitivity range was within that required for human myoglobin determination, following acute myocardial infarction (heart attack). Real-time MyAb-MyAg interaction monitoring, permitted the determination of the binding events in less than one minute.

I. INTRODUCTION

The requirement for the rapid identification of acute myocardial infarction has generated interest in "point-of-care (POC)" devices enabling accurate and reliable diagnostics. POC is a developing concept, providing analysis and diagnosis of clinical conditions from measurements made at the patient's (bed) side [1]. In many cases, just a few drops of blood (~20 µL) in such devices can lead to accurate diagnosis within minutes [2].

The goal of this work, during PhD research, is to examine the influence of interdigitated electrode gap-size on EIS sensitivity with high signal-to-noise ratios for applications in point-of-care cardiac marker analysis [3].

A. Immunosensors.

Biosensors are designed to detect an analyte based upon the use of an immobilized capture probe (e.g. enzyme or antibody) and selectively conjugates a specific target or analyte [4, 5]. The signal generated upon bio-recognition can then be measured in a variety of ways. Electrochemical biosensors have shown promise for applications where miniaturization is crucial to allow production of low cost, single use disposable devices [6].

An immunoassay is defined as an analytical method that uses antibodies or antibody-related reagents to determine sample components [7, 8]. During the last decade, extensive research into assay design and application has led to the development of "user-friendly" immunoassays that are now commonly employed in biomedical and clinical research. Additional progress has recently been made in the area of label-free antibody systems [9].

B. Electrochemical Immunosensors

Electrochemical immunosensor can provide real-time, in-situ monitoring of antibody-antigen interactions.

In general, electrochemical techniques work on several principles. An amperometric sensor is an analytical device that conducts a quantitative measurements based on redox events that are associated with detection of target of interest. Mainly, this target is producing a current whereby its magnitude is proportional to the quantity of target of the selective recognition site [10].

The recognition component of an amperometric sensor usually consists of an electro-active redox species that are composed of chemical or biological test samples integrated with the transducer's electronics [11].

The other type of sensors that measure theses parameters are oxidation-/reduction- based electrochemical reaction. The working principle depend on the fact that when a voltage raised is applied to an electrode in analyte, it causes a current to flow due to electrochemical reactions. This voltage where these reactions took place shows a particular reaction and a measurable potential (potentiometry) [12].

The obtained parameter is called electrical conductance/resistance of the solution. Whenever any electrochemical reaction produce electrical molecule (ions or electrons), the total conductivity/resistivity of this solution varies. Nevertheless, measurements of conductivity have relatively low-sensitivity, and a change in conductivity (conductometry) [13] results from the immune recognition reaction.

In recent years, label-free immunosensor research has focused on biologically-functionalized, one dimensional (1-D) nanostructures [14]. Detection limits of a single virus particle, 10 fM DNA and pM concentration of anti-biotin have been achieved [15, 16].

E. M. Hamad is with the Biomedical Engineering Department, German Jordanian University (phone: +962-6-429-4444 Ext 4433) (e-mail: eyad.hamad@gju.edu.jo).

S.I. Al-Gharabli, is with the Pharmaceutical and Chemical Engineering Department, German Jordanian University, Amman, Jordan (e-mail: samer.gharabli@gju.edu.jo).

J.A. McLaughlin, is with NIBC-School of Engineering, University of Ulster, UK (email: jad.mclaughlin@ulster.ac.uk).

978-1-5386-1311-5/19/$31.00 ©2019 IEEE

C. *Impedimetric biosensors*

Electrical impedance spectroscopy (EIS) is a useful, easy, and sensitive method that has been widely employed in order to measure any amendments at electrode surfaces [17].

Impedance-based biosensors are commonly using the measurement of the interfacial electrical impedance (resistance) under steady-state AC circumstances, by means of sweeping frequency signal with low AC stimuli only (<10 mV), DC bias voltage is zero, to avoid disturbing the probe layer [18].

The magnitude of applied AC current in the electrochemical impedance spectroscopy and its voltage are typically lower than in voltammetry or amperometry [19]. A major advantage of EIS biosensors is their ability to perform label free detection.

II. MATERIALS AND METHODS

A. *Interdigitated Electrodes (IDEs)*

IDEs have fascinated the researcher significantly in recent decades due to the hemispherical diffusion [20, 21], due to their properties in reducing convection effects within the electrodes. Higher sensitivities are achievable in comparison to the classical/conventional electrodes used in electrochemical measurement. It has been presumed based on theoretical calculations that achieving better performance and enhancements can be achieved as dimensions of the electrodes are scaled to sub-micron levels because of reduced penetration of the electric field to the bulk electrolyte [22, 23].

The IDEs used in this study were fabricated at the Tyndall Institute-Ireland as a part of the National Access Programme (NAP). The technique based on e-beam evaporation of gold powder which was evaporated onto Pyrex wafers and then covered with a mask patterned with the electrode design to create the IDES[10] on Pyrex substrate.

The thickness of the Au was maintained at 100 nm with an underlying 10 nm Ti adhesion layer. The Au IDES were flipped face down onto a printed circuit board (PCB). Fig. 1 illustrates the packaged chip and depicts the IDES design. The finger width (W) was kept constant at 5 µm; the gap-size (S) was 10, 7.5, 5 and 2.5 µm respectively.

B. *Electrochemical Impedance Spectroscopy (EIS)*

AC impedance spectra were recorded using a Solartron 1260 impedance gain-phase analyzer with a Solartron 1286 electrochemical interface (Solartron Analytical, UK). EIS measurements were performed on all IDEs in a 5 mM $[Fe(CN6)]^{-3/-4}$ solution with PBS (phosphate buffer saline) (Sigma, UK).

Single frequency measurements were also recorded at 130 Hz and this frequency (130 Hz) was chosen, based on preliminary experiments. The impedance spectra were analyzed and fitted to equivalent circuit models using ZPlot® and ZView® (Scribner Associates Inc., USA).

C. *Preparation of immunosensor*

In order to immobilize antibodies to the gold surface, a self-assembled monolayer (SAM) of alkanethiol was introduced and this provided covalent bonding to react with antibodies [24]. Followed by applying a solution of equal volumes of

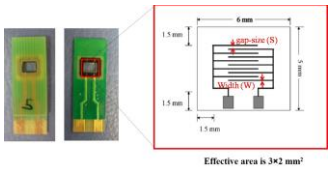

Fig. 1 The packaged chip of IDE on PCB with a schemetic diagram of IDE

4mM of mercapto-1-undecanoic acid (MUA) and 1mM of 11-mercaptoundecanoal (MU) prepared in Ethanol. Thereafter immobilization of human Anti myoglobin (MyAb) (500 µg/mL) (HyTest, Finland) for 30 min. Human Myoglobin (MyAg) (HyTest, Finland) was prepared with a range of concentrations (50 ng/mL) in PBS with Tween20. These antigens were injected onto the prepared immunosensor and the change in impedance (ΔZ) measured as a function of time, over the range 50-300 ng/mL.

III. RESULTS AND DISCUSSION

Before antibody immobilization, impedance measurements were carried out for each bare electrode in 5 mM $[Fe(CN6)]^{-3/-4}$, as reference values, in order to isolate the effect of the gap-size on the produced signal (Fig. 2a).

Theoretically, impedance spectra can be interpreted and analyzed using equivalent circuit (EC) as shown in Fig. 2d. The equivalent circuit is consisting of several electrical elements to determine each electrical component from these spectra, it was noticed that by decreasing the gap-size, both of the key interfacial parameters, charge transfer resistance (Fig. 2a shows a reduction in the diameter of each semicircle, reflecting charge transfer resistance) and double layer capacitance were most sensitive to the reduction. It was noted that the charge transfer resistance had a proportional relationship with gap-size, and that the double layer capacitance was inversely proportional to the gap-size.

By using bare gold IDE sensors, the transferred charge will find more pinholes to penetrate at electrode-electrolyte interface, and consequently, this will reduce R_{ct} by reducing the gap-size. At the same time, it will increase the surface area, resulting with an increase in C_{dl}. Similar results were achieved by different research groups [24, 25].

On the other hand, immobilizing myoglobin antibodies (MyAbs), in conjunction with a SAM of alkanethiol, result in a reduction of the pinholes available on the IDE sensor's

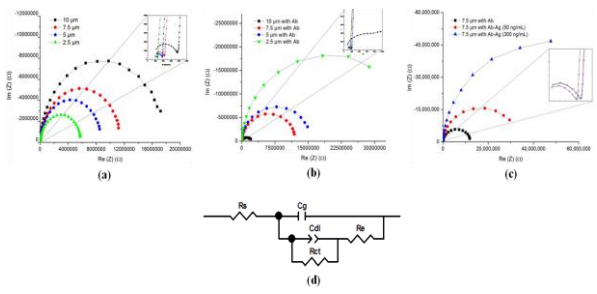

Fig. 2 (a) (b) (c) Nyquist Plot: real and imaginary parts of impedance measurements for different gap-sizes. Inset depicts the high frequency after different concentrations of myoglobin antigen interactions. (d) Equivalent circuit model used

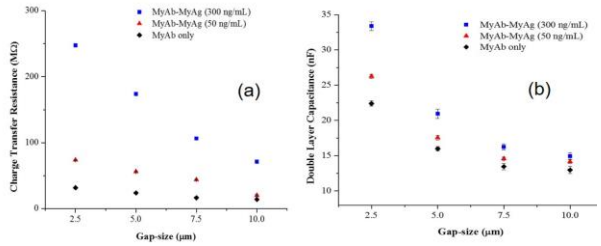

Fig. 3 (a) Illustration of charge transfer resistance (R_{ct}) versus gap size (S) with respect to antibody-antigen interactions. (b) Illustration of double layer capacitance (C_{dl}) versus gap size (S) with respect to antibody-antigen interactions

surface. Therefore, the charge transfer will be hindered at the electrode-electrolyte interface.

An increase in EIS spectra arc diameter was observed following MyAg binding (Fig. 2b). Reducing IDE sensor's gap-size (S) an obvious increment in signal was observed with a substantial influence on both the real and imaginary components of the EIS spectra.

Since antigens and antibodies are usually charged protein molecules, the interaction of Ab-Ag might be affected by the charge applied onto the IDE surface. Therefore, C_{dl} changes that were observed upon formation of the MyAb-MyAg interaction, are potential dependent, which is also gap-size dependent.

Furthermore, increasing in R_{ct} is enabled by reducing the gap-size, whilst using the same concentration of MyAg. Hence, the MyAb-MyAg interaction appears to form an insulation layer at the recognition site, which blocks charge transfer at the electrode-electrolyte interface.

Fig 3a and 3b represent the antibody-antigen interaction effect on R_{ct} and C_{dl} with respect to gap size reduction. R_{ct} and C_{dl} have been increased by decreasing the gap-size of the IDE immunosensor in the case of increasing the concentrations of MyAg.

Ab-Ag interaction clarifies that the antibody immobilization shields the electrode and disturbs the inter-facial electron transfer significantly. As the gap-size reduced, the electron transfer barriers reduced. Regarding to the R_{ct} at the electrode surface, it approves the fact that the electron transfer procedure on the bare gold surface is very fast, whereas construction new layers onto the gold surface, restricted electron transfer process.

The antibody immobilization produced a significant increase of R_{ct}, due to the fact of generating a hydrophobic insulating protein layer onto electrode surface. Followed by Ab-Ag interaction onto the electrode, there is a significant

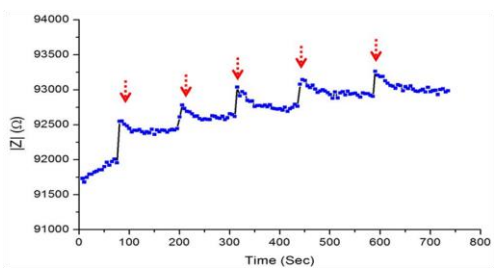

Fig. 5 Bode plot of MyAb-MyAg interaction at 130 Hz vs. time; red arrows represent injection of 50 ng/mL of myoglobin at 2 min.

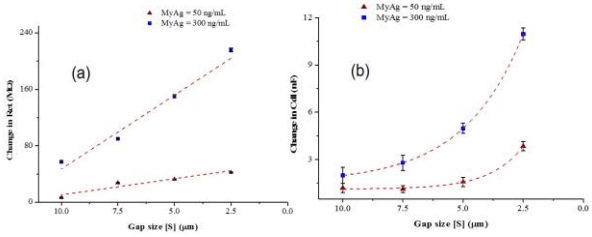

Fig 4 (a) represent the relation between ΔR_{ct} versus S; red triangles demonstrate 50 ng/mL of MyAg, whereas blue squares demonstrate 300 ng/mL of MyAg. (b) represent the relation between ΔC_{dl} versus S; red triangles demonstrate 50 ng/mL of MyAg, whereas blue squares demonstrate 300 ng/mL of MyAg

increase of R_{ct}, reflecting immune detection leads to very significant increments of mass on the electrode surface.

However, significant changes took place after increasing myoglobin antigen (300 ng/mL), Rct increased by 57.3 MΩ and C_{dl} increased by 1.99 nF using S=10 μm IDE immunosensor, whilst R_{ct} increased by 215.77 MΩ and C_{dl} increased by 10.97 nF using S=2.5 μm IDE immunosensor.

Fig. 4a demonstrates the change of the charge transfer resistance (ΔR_{ct}) with respect to the gap size (S) of the IDE immunosensor; it shows a notable increment in ΔR_{ct} after 50 ng/mL of myoglobin antigen interacted with the immobilized myoglobin antigen, although it reveals significant increases in ΔR_{ct} after increasing myoglobin antigens (300 ng/mL).

The changes in R_{ct} for each gap-size can be interpreted due to the reduction of the accessibility of IDE sensor surface of the redox couple in the electrolyte and increasing the thickness of the antibody-antigen layer.

Fig. 4b indicates the change in double layer capacitance (ΔC_{dl}) as a function of gap size (S) for two different myoglobin antigen concentrations; both profiles revealed increasing in ΔC_{dl} by reducing the gap size as a result of forming antibody-antigen layer as anticipated previously. It was assumed that this has occurred, due to the reduction of the thickness of the double layer and minimizing the double layer charging currents where the distance has been reduced.

Real-time monitoring of MyAb-MyAg interactions were conducted at a fixed frequency (130 Hz) by measuring the magnitude of impedance versus time (Fig. 5). The EIS immunosensor exhibited a fast response (within 2-3 seconds) with good reproducibility. EIS measurements at a particular frequency would be another appropriate procedure as concentration dependence. Fig. 6a shows the derived calibration plots that correspond to the change of impedance

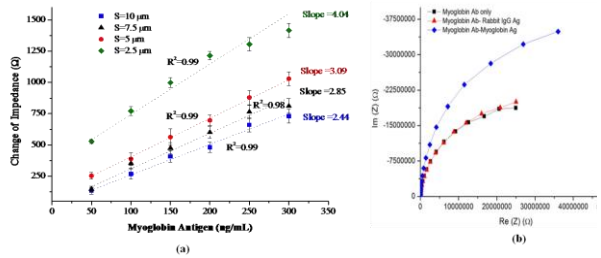

Fig. 6 (a) Calibration curve for each IDE as a function of myoglobin MyAg concentration at 130 Hz (b) sensor selectivity using Rabbit IgG antigen.

as a function of gap-size at the sensing interface with different concentrations of myoglobin antigen.

The effect of IDE finger spacing (gap size) on the change in magnitude of impedance was measured using four sets of IDEs across a range of myoglobin MyAg concentrations (Table I). As the gap-size was reduced, a marked increase in |Z| was observed. Gerwen et. al. predicts from theoretical calculations that reducing the gap size to 1 µm will result in an increased signal-to-noise ratio and enhanced sensitivity, thus concurring with our conclusions [23].

TABLE I. THE CORRESONDING CHANGE OF IMPEDANCE FOR EACH IDE IMMUNOSENSOR WITH DIFFERENT CONCENTRATIONS OF MYOGLOBIN ANTIGEN

Myoglobin Antigen (ng/mL)	Change of Impedance		Change of Impedance		Change of Impedance		Change of Impedance	
	Ω	%	Ω	%	Ω	%	Ω	%
	S=10 µm		S=7.5 µm		S=5 µm		S=2.5 µm	
50	133	26	146	25	253	26	528	16
100	268	40	353	41	388	50	771	37
150	407	46	474	45	562	66	999	40
200	480	42	600	46	697	42	1215	34
250	661	57	764	52	879	57	1306	54
300	730	55	811	58	1030	55	1417	57

A calibration curve was constructed for each pair of IDE electrode (Fig. 6a). A linear relationship was observed between 50-300 ng/mL, demonstrating sensitivity at levels typically required for clinical assays.

The IDE immunosensor selectivity was examined using Rabbit IgG antigen (Fig. 6b). No change in EIS signal was observed, demonstrating that non-specific binding had not occurred. The immunosensor retained its sensitivity towards myoglobin antigens.

In comparison to the work of different research groups [25, 26], the EIS immunosensor obtained lower detection limits without the requirement for a labelling antibody.

IV. CONCLUSIONS

A significant enhancement in EIS immunosensor sensitivity can be achieved by decreasing the gap size (10, 7.5,5 and 2.5 µm) of electrode fingers in IDE arrays. The gap size had a significant effect on charge-transfer-resistance and double-layer-capacitance, which would enhance the sensitivity of the EIS immunosensor. The observed changes of R_{ct} and C_{dl} following binding, related to the effect of the electrical field interaction with MyAb-MyAg binding center.

Both components are influenced by the physical interaction of the MyAb-MyAg but also by the change in electric field, which results from the introduction of surface bound carboxyl anions and ammonium cations present on the surface of the proteins.

The sensor sensitivity range was within that required for human myoglobin determination, following acute myocardial infarction (heart attack). Real-time MyAb-MyAg interaction monitoring, permitted the determination of the binding events in less than one minute.

REFERENCES

[1] A. Schreiber, R. Feldbrügge, G. Key, J. F. C. Glatz, and F. Spener, "An immunosensor based on disposable electrodes for rapid estimation of fatty acid-binding protein, an early marker of myocardial infarction," *Biosensors and Bioelectronics,* Article vol. 12, no. 11, pp. 1131-1137, 1997.

[2] D. R. Thévenot, K. Toth, R. A. Durst, and G. S. Wilson, "Electrochemical biosensors: Recommended definitions and classification," *Biosensors and Bioelectronics,* Article vol. 16, no. 1-2, pp. 121-131, 2001.

[3] E. M. Hamad, "Impedimetric sensors for label-free point-of-care immunoassay cardiac marker systems," PhD, University of Ulster, 2011.

[4] G. Freckmann *et al.*, "System accuracy evaluation of systems for point-of-care testing of blood glucose: A comparison of a patient-use system with six professional-use systems," *Diabetes Technology and Therapeutics,* Note vol. 18, pp. S8-S9, 2016.

[5] D. W. Kemper *et al.*, "Analytical evaluation of a new point of care system for measuring cardiac Troponin I," *Clinical Biochemistry,* Article vol. 50, no. 4-5, pp. 174-180, 2017.

[6] A. Afkhami, P. Hashemi, H. Bagheri, J. Salimian, A. Ahmadi, and T. Madrakian, "Impedimetric immunosensor for the label-free and direct detection of botulinum neurotoxin serotype A using Au nanoparticles/graphene-chitosan composite," *Biosensors and Bioelectronics,* Article vol. 93, pp. 124-131, 2017.

[7] F. Li, Z. Yu, X. Han, and R. Y. Lai, "Electrochemical aptamer-based sensors for food and water analysis: A review," *Analytica Chimica Acta,* Review vol. 1051, pp. 1-23, 2019.

[8] B. Patella, C. Sunseri, and R. Inguanta, "Nanostructured Based Electrochemical Sensors," *Journal of nanoscience and nanotechnology,* Article vol. 19, no. 6, pp. 3459-3470, 2019.

[9] X. Li, J. Ping, and Y. Ying, "Recent developments in carbon nanomaterial-enabled electrochemical sensors for nitrite detection," *TrAC - Trends in Analytical Chemistry,* Review vol. 113, pp. 1-12, 2019.

[10] E. Moore, O. Rawley, T. Wood, and P. Galvin, "Monitoring of cell growth in vitro using biochips packaged with indium tin oxide sensors," *Sensors and Actuators, B: Chemical,* Article vol. 139, no. 1, pp. 187-193, 2009.

[11] E. Martínez-Periñán *et al.*, "Amperometric determination of endoglin in human serum using disposable immunosensors constructed with poly(pyrrolepropionic) acid-modified electrodes," *Electrochimica Acta,* Article vol. 292, pp. 887-894, 2018.

[12] Q. Zhang, A. Prabhu, A. San, J. F. Al-Sharab, and K. Levon, "A polyaniline based ultrasensitive potentiometric immunosensor for cardiac troponin complex detection," *Biosensors and Bioelectronics,* Article vol. 72, pp. 100-106, 2015.

[13] E. Valera, D. Muñiz, and A. Rodríguez, "Fabrication of flexible interdigitated µ-electrodes (FIDµEs) for the development of a conductimetric immunosensor for atrazine detection based on antibodies labelled with gold nanoparticles," *Microelectronic Engineering,* Article vol. 87, no. 2, pp. 167-173, 2010.

[14] K. Ramanathan, M. A. Bangar, M. Yun, W. Chen, N. V. Myung, and A. Mulchandani, "Bioaffinity sensing using biologically functionalized conducting-polymer nanowire," *Journal of the American Chemical Society,* Article vol. 127, no. 2, pp. 496-497, 2005.

[15] I. Burda, C. Baechler, S. Gardin, A. Verma, G. P. Terrasi, and G. Kovacs, "Low-cost scalable printing of carbon nanotube electrodes on elastomeric substrates: Towards the industrial production of EAP transducers," *Sensors and Actuators, A: Physical,* Article vol. 279, pp. 712-724, 2018.

[16] Z. Zhou, W. Xu, Z. Tong, C. W. Lim, and X. Xu, "Theory and modeling of multi-layer carbon nanotube thin film thermoacoustic transducer," *Applied Thermal Engineering,* Article vol. 150, pp. 143-149, 2019.

[17] E. Barsoukov and J. R. Macdonald, *Impedance Spectroscopy: Theory, Experiment, and Applications* (Impedance Spectroscopy: Theory, Experiment, and Applications). 2005, pp. 1-595.

[18] F. Y. Siao, Y. J. Chang, and H. J. Shih, "Label-free immunosensor based on interdigitated electrodes with Ni-Co nanowires," *Micro and Nano Letters,* Article vol. 13, no. 9, pp. 1272-1275, 2018.

[19] O. A. Loaiza *et al.*, "Nanostructured disposable impedimetric sensors as tools for specific biomolecular interactions: Sensitive recognition of concanavalin A," *Analytical Chemistry,* Article vol. 83, no. 8, pp. 2987-2995, 2011.

[20] V. Matylitskaya, S. Kasemann, G. Urban, C. Dincer, and S. Partel, "Electrochemical characterization of nanogap interdigitated electrode arrays for lab-on-a-chip applications," in *ECS Transactions*, 2017, vol. 80, pp. 1295-1308.

[21] S. Partel, S. Kasemann, V. Matylitskaya, C. Thanner, C. Dincer, and G. Urban, "A simple fabrication process for disposable interdigitated electrode arrays with nanogaps for lab-on-a-chip applications," *Microelectronic Engineering,* Article vol. 173, pp. 27-32, 2017.

[22] W. Laureyn *et al.*, "Nanoscaled interdigitated titanium electrodes for impedimetric biosensing," *Sensors and Actuators, B: Chemical,* Article vol. 68, no. 1, pp. 360-370, 2000.

[23] P. Van Gerwen *et al.*, "Nanoscaled interdigitated electrode arrays for biochemical sensors," *Sensors and Actuators, B: Chemical,* Article vol. 49, no. 1-2, pp. 73-80, 1998.

[24] M. M. Billah, H. C. W. Hays, C. S. Hodges, S. Ponnambalam, R. Vohra, and P. A. Millner, "Mixed self-assembled monolayer (mSAM) based impedimetric immunosensors for cardiac troponin i (cTnI) and soluble lectin-like oxidized low-density lipoprotein receptor-1 (sLOX-1)," *Sensors and Actuators, B: Chemical,* Article vol. 173, pp. 361-366, 2012.

[25] S. Ko, B. Kim, S. S. Jo, S. Y. Oh, and J. K. Park, "Electrochemical detection of cardiac troponin I using a microchip with the surface-functionalized poly(dimethylsiloxane) channel," *Biosensors and Bioelectronics,* Article vol. 23, no. 1, pp. 51-59, 2007.

[26] E. Spain *et al.*, "Cardiac Troponin I: Ultrasensitive Detection Using Faradaic Electrochemical Impedance," *ACS Omega,* Article vol. 3, no. 12, pp. 17116-17124, 2018.